Pulse Radiolysis of a Ruthenium(III,III) Oxo-Acetato Dinuclear Complex in Acetonitrile

Taira Imamura,* Akira Kishimoto, Takashi Sumiyoshi,† Kenta Takahashi, Tatsuma Fukumoto, and Yoichi Sasaki

Division of Chemistry, Graduate School of Science, Hokkaido University, Kita-ku, Sapporo 060

†Department of Atomic Science and Nuclear Engineering, Faculty of Engineering, Hokkaido University, Kita-ku, Sapporo 060

(Received May 22, 1995)

Pulse radiolysis of a ruthenium(III,III) oxo-acetato dinuclear complex, $[Ru_2(\mu\text{-}O)(\mu\text{-}CH_3COO)_2(pyridine)_6](PF_6)_2$ (abbr. $Ru_2(33)$), in acetonitrile was studied. Electron-pulse irradiation of deaerated acetonitrile solutions caused one-electron reduction of $Ru_2(33)$ to form $Ru_2(32)$ by the acetonitrile radical anion, $CH_3CN^{\bullet -}$, with a rate constant of 8.0×10^{10} $M^{-1}\,s^{-1}$ (M^{-1}=dm^3 mol^{-1}) at 17 °C. In the solutions containing O_2, $Ru_2(33)$ was competitively reduced by $CH_3CN^{\bullet -}$ and the superoxide ion, O_2^-, with a rate constant of 1.1×10^{10} $M^{-1}\,s^{-1}$, to form $Ru_2(32)$. This was reoxidized by the peroxyl radical, $^{\bullet}O_2CH_2CN$, with a rate constant of 7.5×10^9 $M^{-1}\,s^{-1}$ to regenerate the parent complex of $Ru_2(33)$. The reaction scheme is discussed in comparison with the results for the ruthenium(III,III,III) trinuclear complex, $[Ru_3(\mu_3\text{-}O)(\mu\text{-}CH_3COO)_6(pyridine)_3]PF_6$ (abbr. $Ru_3(333)$), reported previously.

Radiolysis of the acetonitrile liquid phase produces the acetonitrile radical cation $CH_3CN^{\bullet +}$ and electron e^-, which react with CH_3CN to give the neutral radical $^{\bullet}CH_2CN$ and the acetonitrile radical anion $CH_3CN^{\bullet -}$ respectively.[1,2] The acetonitrile radical anion $CH_3CN^{\bullet -}$ is a strong reducing agent. When the solution contains O_2, $CH_3CN^{\bullet -}$ reacts with it to give the secondary reducing agent of superoxide ion, O_2^-,[1,3] having a half wave-potential of O_2/O_2^- at −0.65 V vs. NHE (−0.87 V vs. Ag/AgCl),[4] and $^{\bullet}CH_2CN$ gives $^{\bullet}O_2CH_2CN$ which has oxidizing ability.[3,5]

We previously reported the radiolytic reactions of the ruthenium(III,III,III) oxo-acetato trinuclear pyridine complex, $[Ru_3(\mu_3\text{-}O)(\mu\text{-}CH_3COO)_6(pyridine)_3]PF_6$ (abbr. $Ru_3(333)$, Fig. 1) in acetonitrile.[4] $Ru_3(333)$ has reversible electrochemical multistep one-electron redox behavior.[6—9] Irradiation of deaerated acetonitrile $Ru_3(333)$ solutions induced one-electron reduction of the trinuclear $Ru_3(333)$ center by $CH_3CN^{\bullet -}$ to form $Ru_3(332)$. In aerated solutions, $Ru_3(333)$ was competitively reduced by both $CH_3CN^{\bullet -}$ and O_2^-, followed by the regeneration of $Ru_3(333)$.[4] We also proposed a comprehensive reaction mechanism. This mechanism involves intrinsic reaction parameters of solvent acetonitrile and can be applied to other radiolytic reaction systems of acetonitrile solutions.

The ruthenium(III, III) dinuclear pyridine complex $[Ru_2(\mu\text{-}O)(\mu\text{-}CH_3COO)_2(pyridine)_6](PF_6)_2$ (abbr. $Ru_2(33)$, Fig. 1) has a similar structure to $Ru_3(333)$ in the sense that two ruthenium ions are bridged by one oxide and two acetato ions.[10—12] The bridging structure, $M_2(\mu\text{-}O)(\mu\text{-}RCOO)_2$, is found in some metalloenzymes such as methemerythrin.[13,14] Thus $Ru_2(33)$ is an attractive complex on the bases of not only purely chemical but also bioinorganic aspects. There are several differences between $Ru_2(33)$ and $Ru_3(333)$. The charges for these complex ions are 2+ and 1+ and the numbers of coordinating pyridine are 6 and 3 respectively. In a recent report on pulse radiolysis of the ruthenium(II) polypyridine complexes in H_2O, the rate constants for the reaction between e^-_{aq} and the complexes increased linearly with the number of ligands coordinated to the central ruthenium ions.[15] The reduction of $Ru_2(33)$ would be favorable then as far as the number of pyridine and charge of complex ions are concerned, provided that the same mechanism operates as $Ru_3(333)$. Contrary to the above expectations, the half-wave potential of $Ru_2(33)/Ru_2(32)$ observed at −0.06 V vs. NHE (−0.85 V vs. $Ag/AgClO_4$)[12] suggested disadvantages for the $Ru_2(33)$ reduction in comparison to the $Ru_3(333)$ system ($Ru_3(333)/Ru_3(332)$; +0.47 V vs. NHE).[9]

In this report, the kinetics and mechanism of the $Ru_2(33)$ system are discussed in comparison to those of the corresponding $Ru_3(333)$ system. In addition, the absorption spectrum of $Ru_2(32)$ obtained by pulse radiolysis is discussed, because no reliable absorption spectrum of $Ru_2(32)$ has been reported so far.

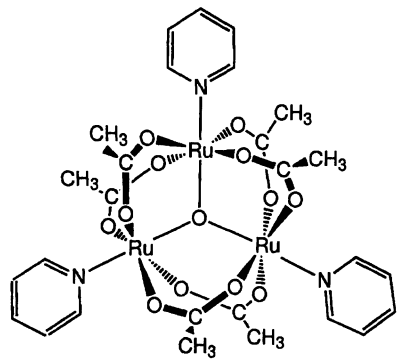

$[Ru_3(\mu_3\text{-}O)(\mu\text{-}CH_3COO)_6(pyridine)_3]^{+}$
≡ $Ru_3(333)$

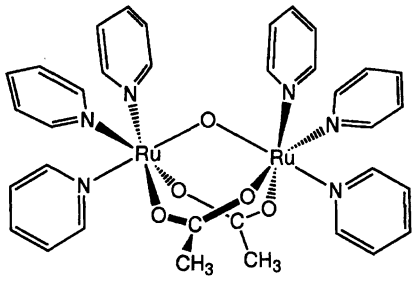

$[Ru_2(\mu\text{-}O)(\mu\text{-}CH_3COO)_2(pyridine)_6]^{2+}$
≡ $Ru_2(33)$

Fig. 1. Structures of the $Ru_3(333)$ and $Ru_2(33)$ complexes.

Experimental

Apparatus. Electronic spectra for statistical measurements were recorded on a Hitachi 340 or a JASCO Ubest-30 spectrophotometer. The pulse radiolysis apparatus was similar to that reported previously.[4,16] A 45 MeV electron-pulse from an S-band linear accelerator (Mitsubishi) was applied to the acetonitrile sample solutions at 17 °C. The half-width of the pulse was 10 ns. Optical cells of path length 1.0 cm were used. The absorbed doses per pulse were determined by KSCN dosimetry[17] and varied from 38 to 68 Gy. Irradiation with an absorbed dose of 50 Gy per pulse of neat acetonitrile or the acetonitrile solutions of $Ru_2(33)$ produced 8.2×10^{-6} M (M=mol dm^{-3}) of reducing species of $CH_3CN^{\bullet-}$, as calculated by using G (radiation chemical yield) value of 0.21 μmol J^{-1}.[4] The reaction processes were followed spectrophotometrically in the UV-vis region using analyzing light from a 1 kw xenon arc lamp. Rate constants were determined by iterative computer simulations of the optical density vs. time profiles obtained at various experimental conditions, using the Runge–Kutta method.[18] The errors of the rate constants thus obtained were within about ±15%.

Materials. The complex $[Ru_2(\mu\text{-}O)(\mu\text{-}CH_3COO)_2(pyridine)_6](PF_6)_2$ was prepared by the reported method and identified by elemental analysis and ^{1}H NMR, IR, and UV-vis spectral measurements.[10—12] The pyridine ligands coordinated to the ruthenium ions do not dissociate in acetonitrile solutions.[10—12] Acetonitrile of nonfluorescent spectral grade was purchased from Dojin and used without further purification unless otherwise specified. The same batch of acetonitrile was used throughout this work to maintain the constancy of impurity effects.[19] Sample solutions for pulse radiolysis were bubbled with argon or oxygen and sealed with a Teflon® bulb prior to irradiation. Otherwise the sample solutions were prepared and degassed on the vacuum line where the solution cells were sealed. Argon and oxygen of ultrahigh purity were obtained from Hoxan and Nipponsanso respectively. Potassium superoxide, KO_2, from ICN Pharmaceuticals was used for the direct reduction of $Ru_2(33)$ without further purification. The reduction was followed spectrophotometrically by the addition of excess of KO_2 powder to the $Ru_2(33)$ acetonitrile solutions, which were degassed in advance and kept in the vacuum line.

Results and Discussion

Radiolysis of Acetonitrile. Pulse irradiation of neat acetonitrile gave broad weak absorption bands in the visible region, with a maximum around 500 nm within 50 ns, due to the formation of $CH_3CN^{\bullet-}$ and/or $(CH_3CN)_2^{\bullet-}$, as was reported by Bell et al.[1] As in the previous report,[4] we represented both these reducing species as $CH_3CN^{\bullet-}$, since the difference in the reactivity of the two species has not been yet thoroughly clarified. Thus, the evaluated reactivity would represent those of both species. In deaerated neat acetonitrile, the following mechanism has been proposed:[1]

$$CH_3CN \rightsquigarrow CH_3CN^{\bullet+} + e^- \quad (1)$$

$$e^- + CH_3CN \rightarrow CH_3CN^{\bullet-} \quad (2)$$

$$CH_3CN^{\bullet+} + CH_3CN \rightarrow {}^{\bullet}CH_2CN + CH_3CNH^+ \quad (3)$$

$$CH_3CN^{\bullet-} \rightarrow \text{product} \quad (4)$$

The spontaneous decay rate constant k_4 (the subscript shows the equation number) of the radical species is evaluated to be $(2.0\pm0.3)\times10^6$ s^{-1} from the decay curve of $CH_3CN^{\bullet-}$. Although this value is smaller than the previously reported value, $(3.0\pm0.2)\times10^6$ s^{-1},[4] it is in the range of the reported rate constants, 7.9×10^5 to 1.7×10^7 s^{-1}.[1,20] This result indicated that the impurity content of acetonitrile used for the present work was less than that used for the $Ru_3(333)$ system. Air- or oxygen-saturated acetonitrile showed no absorption bands in the visible region, as a result of the rapid reaction of $CH_3CN^{\bullet-}$ with O_2 as described in the next section.

Radiolysis of Air- or Oxygen-Saturated Solutions of $Ru_2(33)$. $Ru_2(33)$ in acetonitrile has absorption peaks at 325 and 583 nm with respective molar absorptivities of 16700 and 9700 M^{-1} cm^{-1}, as shown in Fig. 2. Electron pulse irradiation of air- or oxygen-saturated (7×10^{-3} M)[1] solutions of $Ru_2(33)$ decreased the absorbance at 583 nm, with concomitant increase of the absorbance at 430 nm, as shown in the difference absorption spectral change in Fig. 3. This spec-

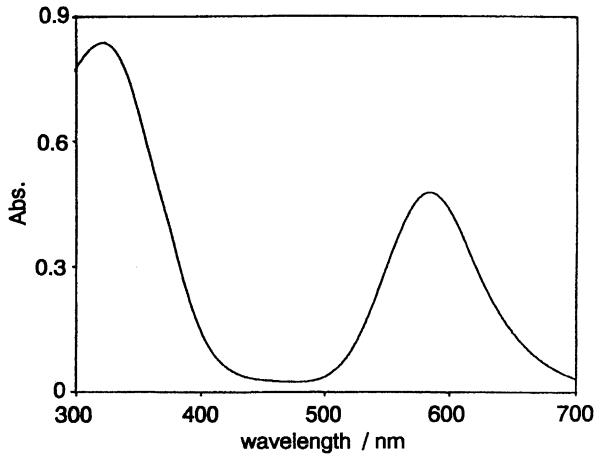

Fig. 2. Visible absorption spectrum of 4.4×10^{-5} M of $Ru_2(33)$ in acetonitrile.

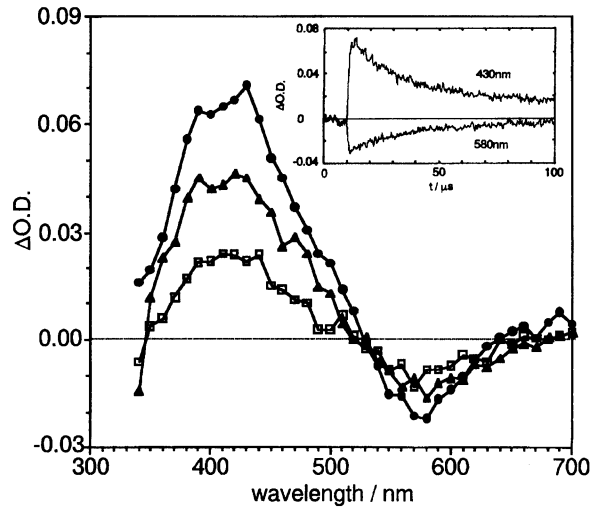

Fig. 3. Difference absorption spectra at 200 ns (□), 500 ns (▲), and 4 μs (●) after pulse irradiation of the 5.95×10^{-5} M of $Ru_2(33)$ oxygen-saturated acetonitrile solution at 17 °C. The absorbed dose per pulse was 51 Gy. The inset shows the changes in the difference absorbances at 430 and 580 nm within 100 μs after pulse irradiation.

tral change has isosbestic points at 345 and 530 nm on the zero difference absorbance base line. As in the case of the $Ru_3(333)$ reaction systems, this absorbance change should be ascribed to the formation of $Ru_2(32)$ by one-electron reduction. The apparent rates of the reactions decreased with increasing the concentration of O_2. The effects of the concentration of O_2 on the reaction rate indicated that O_2^- also reduced $Ru_2(33)$ as well as $CH_3CN^{\bullet-}$. The progress of the reduction of $Ru_2(33)$ by O_2^- was supported by the half-wave potentials of −0.65 V (vs. NHE) for O_2/O_2^-,[4] and of −0.06 V for $Ru_2(33)/Ru_2(32)$[12] and the direct reduction of $Ru_2(33)$ with KO_2 (vide infra).

After the absorbance at 430 nm reached its maximum, the absorbance decreased with concomitant increase in the absorbance at 583 nm toward the zero baseline: this revealed the regeneration of the parent complex of $Ru_2(33)$. This spectral change also had isosbestic points at 345 and 530 nm. The reoxidation reaction was completed within 500 μs. Such recovery was also observed for the $Ru_3(333)$ reaction system.[4] The reactions for air- or oxygen-saturated solutions should be denoted in Eqs. 5, 6, 7, 8, 9, 10, 11, 12, and 13.

$$CH_3CN^{\bullet-} + Ru_2(33) \rightarrow CH_3CN + Ru_2(32) \quad (5)$$

$$CH_3CN^{\bullet-} + O_2 \rightarrow CH_3CN + O_2^- \quad (6)$$

$$CH_3CN + O_2^- \rightarrow CH_3CN^{\bullet-} + O_2 \quad (7)$$

$$O_2^- + Ru_2(33) \rightarrow O_2 + Ru_2(32) \quad (8)$$

$$O_2^- \rightarrow \text{product} \quad (9)$$

$$^{\bullet}CH_2CN + O_2 \rightarrow {}^{\bullet}O_2CH_2CN \quad (10)$$

$$O_2^- + {}^{\bullet}O_2CH_2CN \rightarrow O_2 + {}^{-}O_2CH_2CN \quad (11)$$

$${}^{\bullet}O_2CH_2CN + Ru_2(32) \rightarrow {}^{-}O_2CH_2CN + Ru_2(33) \quad (12)$$

$${}^{\bullet}O_2CH_2CN \rightarrow \text{product} \quad (13)$$

These overall reaction features are the same to those of the $Ru_3(333)$ system, i.e., $Ru_2(33)$ is competitively reduced by O_2^- and $CH_3CN^{\bullet-}$ to form the same $Ru_2(32)$ complex, followed by the regeneration of the parent $Ru_2(33)$ complex by the reaction of $Ru_2(32)$ with the peroxyl radical, ${}^{\bullet}O_2CH_2CN$, as shown in Scheme 1.

Radiolysis of Argon-Saturated or Degassed Solutions of $Ru_2(33)$. Upon irradiation with an electron-pulse, the argon-saturated or degassed solutions of $Ru_2(33)$ showed a rapid spectral change. Transient difference spectra at the initial stage of the reaction were

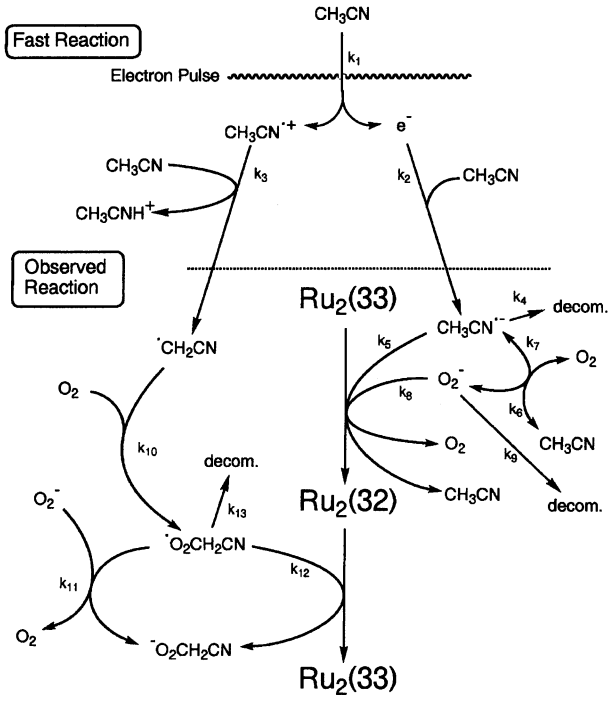

Scheme 1.

essentially the same as those of the air- or oxygen-saturated solution systems, as shown in Fig. 4, i.e., $Ru_2(33)$ was reduced by $CH_3CN^{\bullet -}$ to form $Ru_2(32)$. However, two different features were observed. One is no regeneration of $Ru_2(33)$ was observed within 1 ms after the formation of $Ru_2(32)$. This is because of the absence of the peroxyl radical, $^{\bullet}O_2CH_2CN$.[3,5] The other is the appearance of extra apparent isosbestic point at 525 nm observed above the zero baseline. The isosbestic point indicated the existence of some chemical species which is stable during the course of the reaction.

Although the radical anion $CH_3CN^{\bullet -}$ in neat acetonitrile has a broad absorption band around 500 nm in the absence of oxygen, the appearance of the isosbestic point around 525 nm should be ascribed not only to $CH_3CN^{\bullet -}$ but also to some unknown chemical species. The reason is that the absorbance at the isosbestic point is a little larger than the absorbance at 525 nm of $CH_3CN^{\bullet -}$ itself. In addition, $CH_3CN^{\bullet -}$ once formed must be consumed to reduce $Ru_2(33)$ especially at the final stage of the reaction. In the argon or degassed systems, $^{\bullet}CH_2CN$ lives longer without O_2 and thus has a chance to react further before the reaction with $Ru_2(33)$. Thus we tentatively ascribed the appearance of the apparent isosbestic point in the argon or degassed systems to the formation of the unknown species, e.g., a small amount of some polymers derived from $^{\bullet}CH_2CN$ or $CH_3CN^{\bullet +}$. It seems that the unknown species gives a weak and broad absorption around 500 nm.[21]

Yield of $Ru_2(32)$. The amount of $Ru_2(32)$ formed upon electron-pulse irradiation of argon-, air-, or oxygen-saturated solutions was evaluated from the maximum absorbances reached at 450 nm. The maximum absorbances increased with increasing initial concentration of $Ru_2(33)$ and approached a constant value. The plot of the reciprocal maximum absorbance, ΔOD^{-1}, normalized to 50 Gy, at 450 nm vs. the reciprocal initial concentration of $Ru_2(33)$, $[Ru_2(33)]^{-1}$, for argon- or air-saturated solutions gave almost straight lines, as shown in Fig. 5. The intercepts ΔOD^{-1}_{max} were the reciprocal maximum absorbances at infinite concentration of $Ru_2(33)$. Figure 5 shows that the intercepts of argon- and air-saturated solutions are slightly different. The difference could be due to the formation of the unknown species in argon-saturated solutions. We consider that the intercepts are practically identical. Therefore we conclude that only $CH_3CN^{\bullet -}$ and O_2^- acted as reducing agents, i.e., the neutral radical $^{\bullet}CH_2CN$ did not take part in the $Ru_2(33)$ reductions. From the value of the intercept for air-saturated solutions, the difference molar absorptivity between $Ru_2(32)$ and $Ru_2(33)$ at 450 nm was determined to be $\Delta\varepsilon = 15170\ M^{-1}\,cm^{-1}$ using Eq. I, where G, Da, ρ, and l were the radiation chemical yield ($\mu mol\,J^{-1}$), the absorbed dose per pulse (Gy), density of CH_3CN ($g\,cm^{-3}$), and the path length of optical cell (cm) respectively. The maximum concentration of $Ru_2(32)$ may correspond to the concentration of $CH_3CN^{\bullet -}$ produced by pulse irradiation.

$$\Delta\epsilon = (\Delta OD_{max} \times 10^6)/(Da \times \rho \times G \times l) \qquad (I)$$

Plots of ΔOD^{-1}_{max} vs. $[Ru_2(33)]^{-1}$ for oxygen-saturated systems also gave a straight line having a different slope but the same intercept as that for the air-saturated solutions. Evaluation of ΔOD_{max} at UV-vis region for oxygen-saturated solutions afforded the absorption spec-

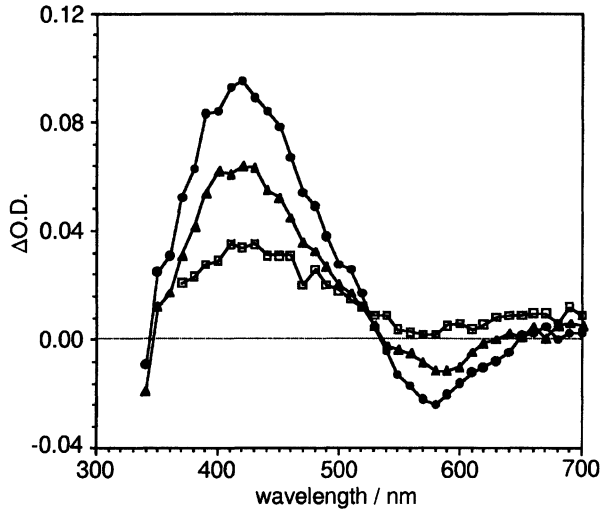

Fig. 4. Difference absorption spectra at 50 ns (□), 150 ns (▲), and 3 μs (●) after pulse irradiation of the 5.42×10^{-5} M of $Ru_2(33)$ degassed acetonitrile solution at 17 °C. The absorbed dose per pulse was 55 Gy.

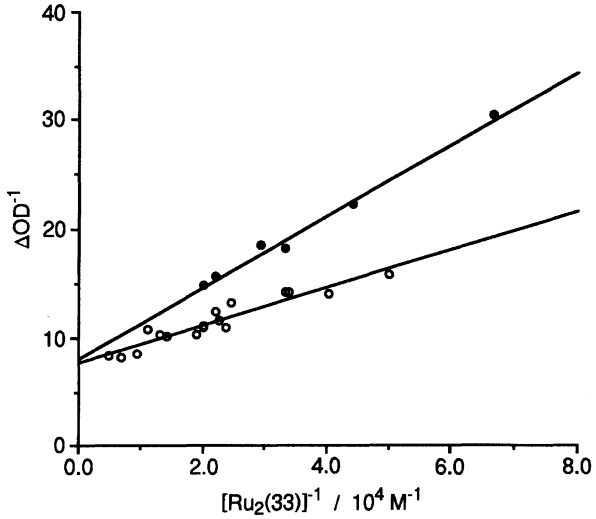

Fig. 5. Plots of the reciprocal maximum absorbance at 450 nm vs. the reciprocal initial concentration of $Ru_2(33)$ for the $Ru_2(33)$ reduction to $Ru_2(32)$ induced by pulse radiolysis of air-saturated (●) and argon-saturated (○) acetonitrile solutions at 17 °C. The absorbed dose per pulse was normalized to 50 Gy.

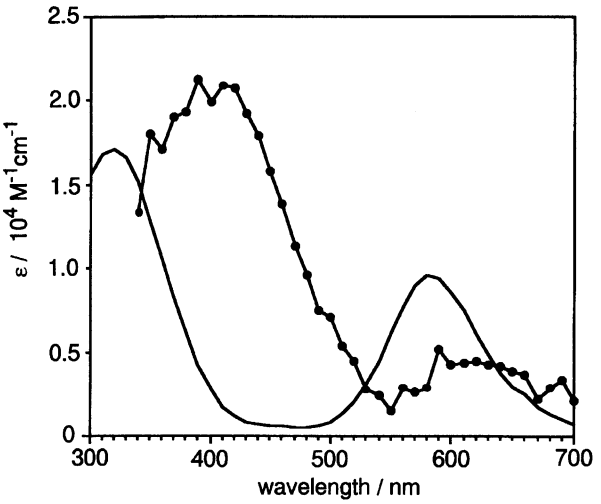

Fig. 6. Absorption spectra of $Ru_2(32)$ (●), obtained by pulse radiolysis and the parent complex of $Ru_2(33)$ (—).

trum of $Ru_2(32)$, as shown in Fig. 6.

Kinetics. In deaerated solutions, the apparent reduction rate constants, k_{obsd}, of $Ru_2(33)$ depend only on the reaction rate constants of k_4 and k_5, i.e., $k_{obsd} = k_4 + k_5[Ru_2(33)]$, because of the absence of reactions 6—13. The values of k_{obsd} were, however, scattered, as shown in Fig. 7. The value of k_5 was tentatively estimated to be $(8\pm1)\times10^{10}$ $M^{-1}s^{-1}$ from the slope of the plots. The confident rate constant was analyzed by Eq. II.

$$(\Delta OD)^{-1} = (\Delta OD_{max})^{-1} + (\Delta OD_{max})^{-1}(k_4/k_5)([Ru_2(33)])^{-1} \quad (II)$$

The plots of ΔOD^{-1} (corrected by subtracting the absorbance by unknown species) vs. $[Ru_2(33)]^{-1}$ gave a straight line. As described in the former section, the

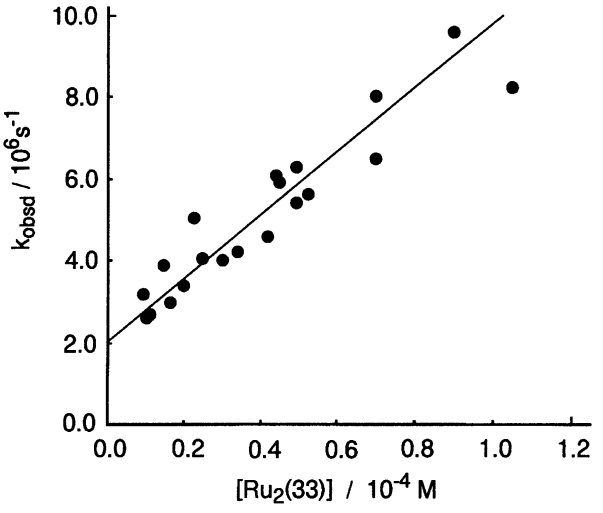

Fig. 7. Plots of apparent rate constants, k_{obsd} (grow-in at 450 nm) obtained kinetically, vs. $[Ru_2(33)]$, for the argon-saturated systems at 17 °C.

decay rate constant of $CH_3CN^{\bullet-}$, k_4 was evaluated to be $(2.0\pm0.3)\times10^6$ s^{-1} from the absorbance changes with time for the argon-saturated neat acetonitrile solutions. The second order rate constant, k_5, was finally evaluated from the slope to be $(8.0\pm0.8)\times10^{10}$ $M^{-1}s^{-1}$ using the k_4 value. The value was in the range of reported diffusion-controlled rate constants: 3.3×10^{10} to 1.2×10^{11} $M^{-1}s^{-1}$.[1,22,23]

These values, k_4 and k_5, were used to evaluate the rate constants of k_8, k_9, k_{12}, and k_{13} by Runge–Kutta method[18] applied for five Eqs. III to VII. The values of other rate constants k_6, k_7, k_{10}, and k_{11} were fixed to be the same as the previous values of the $Ru_3(333)$ systems.

$$d[CH_3CN^{\bullet-}]/dt = -k_4[CH_3CN^{\bullet-}] - k_5[CH_3CN^{\bullet-}][Ru_2(33)] - k_6[CH_3CN^{\bullet-}][O_2] + k_7[CH_3CN][O_2^-] \quad (III)$$

$$d[Ru_2(32)]/dt = k_5[CH_3CN^{\bullet-}][Ru_2(33)] + k_8[O_2^-][Ru_2(33)] - k_{12}[Ru_2(32)][^{\bullet}O_2CH_3CN] \quad (IV)$$

$$d[O_2^-]/dt = k_6[CH_3CN^{\bullet-}][O_2] - k_7[CH_3CN][O_2^-] - k_9[O_2^-] - k_8[O_2^-][Ru_2(33)] - k_{11}[O_2^-][^{\bullet}O_2CH_3CN] \quad (V)$$

$$d[^{\bullet}CH_2CN]dt = -k_{10}[^{\bullet}CH_2CN][O_2] \quad (VI)$$

$$d[^{\bullet}O_2CH_3CN]/dt = k_{10}[^{\bullet}CH_2CN][O_2] - k_{11}[O_2^-][^{\bullet}O_2CH_3CN] - k_{13}[^{\bullet}O_2CH_3CN] - k_{12}[Ru_2(32)][^{\bullet}O_2CH_3CN] \quad (VII)$$

Table 1 summarizes the rate constants of the $Ru_2(33)$ and $Ru_3(333)$ systems. Figure 8 showed simulation curves using the values. The curves reproduced well the experimental curves under various conditions. These

Table 1. Reaction Rate Constants of the Irradiated $Ru_2(33)$ and $Ru_3(333)$ Acetonitrile Systems at 17 and 14 °C Respectively

	$Ru_2(33)$[a]	$Ru_3(333)$[b]
k_4	$(2.0\pm0.3)\times10^6$ s^{-1}	$(3.0\pm0.2)\times10^6$ s^{-1}
k_5	$(8.0\pm0.8)\times10^{10}$ $M^{-1}s^{-1}$	$(6.1\pm0.6)\times10^{10}$ $M^{-1}s^{-1}$
k_6	$(1.0\pm0.1)\times10^{11}$ $M^{-1}s^{-1}$	
k_7	$(2.0\pm0.2)\times10^6$ $M^{-1}s^{-1}$	
k_8	$(1.1\pm0.1)\times10^{10}$ $M^{-1}s^{-1}$	$(3.5\pm0.2)\times10^9$ $M^{-1}s^{-1}$
k_9	$(5.0\pm0.8)\times10^5$ s^{-1}	$(6\pm1)\times10^5$ s^{-1}
k_{10}	$(1.1\pm0.1)\times10^9$ $M^{-1}s^{-1}$	
k_{11}	$(2.8\pm0.2)\times10^{10}$ $M^{-1}s^{-1}$	
k_{12}	$(7.5\pm0.8)\times10^9$ $M^{-1}s^{-1}$	$(2.7\pm0.2)\times10^9$ $M^{-1}s^{-1}$
k_{13}	$(1.0\pm0.1)\times10^4$ s^{-1}	$(2.0\pm0.2)\times10^4$ s^{-1}

a) This work. b) Ref. 4.

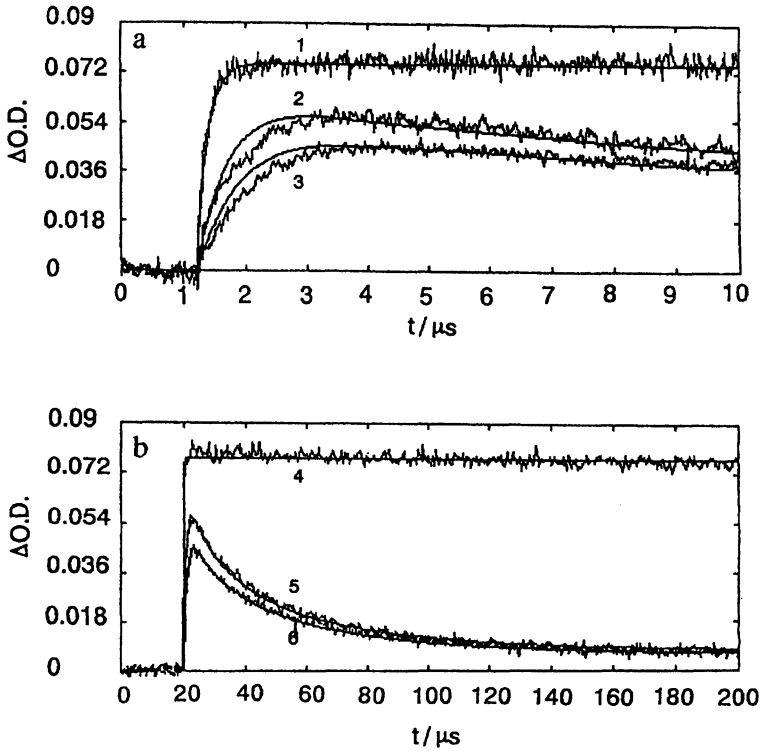

Fig. 8. Absorbance changes at 450 nm vs. time for the reduction of $Ru_2(33)$ to $Ru_2(32)$ induced by pulse radiolysis of acetonitrile solutions at 17 °C under various conditions. Solid lines are the absorption curves simulated using the rate constants in Table 1. (a) 1, 2, and 3 are the absorption curves within 10 μs respectively for the argon-, air-, and oxygen-saturated solutions of $[Ru_2(33)]=4.98\times10^{-5}$ M. (b) 4, 5, and 6 are the curves within 200 μs for the same systems with 1, 2, and 3, respectively.

values also indicated that ca. 73% of $Ru_2(33)$ in oxygen-saturated solutions is reduced by O_2^-.

As described in the introduction section, $Ru_2(33)$ is not easily reduced electrochemically in comparison to $Ru_3(333)$. However, Table 1 reveals that all the rate constants of k_5, k_8, and k_{12} for the $Ru_2(33)$ system are larger than those for the $Ru_3(333)$ system. The results suggest that another factors such as the charge on the complex ions or the number of pyridine ligands coordinated to the ruthenium metal ions are more important to determine the reaction rates than the redox potentials for these dinuclear and trinuclear reaction systems. The results may imply that the initial attack of active species on the pyridine ligands is important.

Reaction with Potassium Superoxide. The direct reduction of $Ru_2(33)$ by O_2^- was followed by the addition of excess KO_2 powder to the $Ru_2(33)$ acetonitrile solutions. The reduction immediately gave $Ru_2(32)$. As expected from the k_8 value in Table 1, the visible spectral change was too fast to follow spectrophotometrically using a cell connected to a vacuum line. Only a point of intersection around 530 nm was seen between the spectra of the formed $Ru_2(32)$ and the parent $Ru_2(33)$ as shown in Fig. 9. The spectrum of $Ru_2(32)$ is similar to that obtained by pulse radiolysis. In addition, the spectrum of $Ru_2(32)$ thus obtained showed a broad and weak absorption band around 900 nm. The formation of $Ru_2(32)$ was followed by successive two-step spectral changes due to unknown reactions, i.e., absorbance around 440 nm was increased with an isosbestic point at 490 nm with the $Ru_2(32)$ spectrum (the second stage, b→c in Fig. 9). The spectrum thus obtained changed again with time to the spectrum with the peaks at 350 and 620 nm (the third

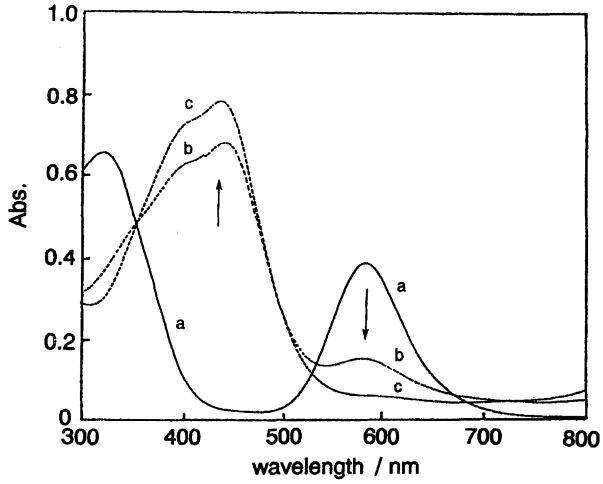

Fig. 9. Absorption spectra of the 4.1×10^{-5} M $Ru_2(33)$ acetonitrile solution at 0 (a—), 2 (b····), and 7 (c–·–) min after direct addition of KO_2.

stage). The last spectral change has an isosbestic point at 540 nm. These results suggest that $Ru_2(32)$ is very unstable in the acetonitrile solutions containing large amounts of reducing agents. Although the products in the second and third stages of the reactions under the conditions containing excess KO_2 have not been characterized yet, the formation of $Ru_2(32)$ by the reaction of $Ru_2(33)$ with O_2^- was evident.

Conclusion

The scheme of the radiolytic reactions of the ruthenium trinuclear $Ru_3(333)$ system proposed by our previous paper was proved to be applicable to the $Ru_2(33)$ system. $Ru_2(33)$ in the presence of oxygen was reduced competitively by $CH_3CN^{\bullet -}$ and O_2^- to give the $Ru_2(32)$ complex. The UV-vis spectral change afforded a spectrum of $Ru_2(32)$. $Ru_2(32)$ thus formed was reoxidized to the parent $Ru_2(33)$ complex. In argon-saturated systems, $Ru_2(32)$ was formed by the reaction of $Ru_2(33)$ with $CH_3CN^{\bullet -}$. In comparison to the $Ru_3(333)$ reaction system, all the reduction rate constants for $Ru_2(33)$ are larger, though the half-wave potential of $Ru_2(33)/Ru_2(32)$ suggested the difficulty of the reduction. The results suggest that other functions such as the number of pyridine ligands coordinated to the ruthenium ions or the total charge of the complexes are influential on the rates.

The authors are very grateful to Professor Sadashi Sawamura and Messrs. Hiroaki Tanida and Koichi Sato for their help in operating the LINAC. This work was partly supported by a Grant-in-Aid for Scientific Research No. 06804034 from the Ministry of Education, Science and Culture, the 1993 Suhara Memorial Foundation, and the 1994 Kawasaki Steel 21st Century Foundation.

References

1) I. P. Bell, M. A. J. Rodgers, and H. D. Burrows, *J. Chem. Soc., Faraday Trans. 1*, **73**, 315 (1977).

2) J. L. Baptista and H. D. Burrows, *J. Chem. Soc., Faraday Trans. 1*, **70**, 2066 (1974).

3) T. H. Tran-Thi, A. M. Koulkes-Pujo, L. Gilles, M. Genies, and J. Sutton, *Radiat. Phys. Chem.*, **15**, 209 (1980).

4) T. Imamura, T. Sumiyoshi, K. Takahashi, and Y. Sasaki, *J. Phys. Chem.*, **97**, 7786 (1993).

5) S. Mosseri, P. Neta, and D. Meisel, *Radiat. Phys. Chem.*, **36**, 683 (1990).

6) J. A. Baumann, D. J. Salmon, S. T. Wilson, T. J. Meyer, and W. E. Hatfield, *Inorg. Chem.*, **17**, 3342 (1978).

7) a) H. E. Toma and C. J. Cunha, *Can. J. Chem.*, **67**, 1632 (1989); b) H. E. Toma and M. A. L. Olive, *Polyhedron*, **13**, 2647 (1994).

8) a) A. Spencer and G. Wilkinson, *J. Chem. Soc., Dalton Trans.*, **1972**, 1570; **1974**, 786; b) J. A. Baumann, S. T. Wilson, D. J. Salmon, P. L. Hood, and T. J. Meyer, *J. Am. Chem. Soc.*, **101**, 2916 (1979); c) H. E. Toma, C. J. Cunha, and C. Cipriano, *Inorg. Chim. Acta*, **154**, 63 (1988); d) S. Cosnier, A. Deronzier, and A. Llobet, *J. Electroanal. Chem.*, **280**, 213 (1990); e) D. Akashi, H. Kido, Y. Sasaki, and T. Ito, *Chem. Lett.*, **1992**, 143; f) M. Abe, Y. Sasaki, T. Yamaguchi, and T. Ito, *Bull. Chem. Soc. Jpn.*, **65**, 1585 (1992); g) H. E. Toma, F. M. Matsumoto, and C. Cipriano, *J. Electroanal. Chem.*, **346**, 261 (1993); h) H. E. Toma and A. D. P. Alexiou, *Electrochim. Acta*, **38**, 975 (1993).

9) Y. Sasaki, A. Tokiwa, and T. Ito, *J. Am. Chem. Soc.*, **109**, 6341 (1987).

10) T. Fukumoto, K. Umakoshi, and Y. Sasaki, unpublished results.

11) Y. Sasaki, M. Suzuki, A. Tokiwa, M. Ebihara, T. Yamaguchi, C. Kabuto, and T. Ito, *J. Am. Chem. Soc.*, **110**, 6251 (1988).

12) Y. Sasaki, M. Suzuki, A. Nagasawa, A. Tokiwa, M. Ebihara, T. Yamaguchi, C. Kabuto, T. Ochi, and T. Ito, *Inorg. Chem.*, **30**, 4903 (1991).

13) a) S. J. Lippard, *Angew. Chem., Int. Ed. Engl.*, **27**, 344 (1988); b) K. Wieghardt, *Angew. Chem., Int. Ed. Engl.*, **28**, 1153 (1989).

14) L. Que, Jr., and A. E. True, *Progr. Inorg. Chem.*, **38**, 97 (1989).

15) B. J. Parsons, P. C. Beaumont, S. Navaratnam, W. D. Harrison, T. S. Akasheh, and M. Othman, *Inorg. Chem.*, **33**, 157 (1994).

16) T. Suzuki, T. Imamura, T. Sumiyoshi, M. Katayama, and M. Fujimoto, *Inorg. Chem.*, **29**, 1123 (1990).

17) E. M. Fielden and N. W. Holm, "Manual on Radiation Dosimetry," ed by N. W. Holm and R. J. Berry, Marcel Dekker, New York (1990), p. 288.

18) H. Margenau and G. M. Murphy, "The Mathematics of Physics and Chemistry," D. van Nostrand Co., New York (1955).

19) Acetonitrile containing less than 5×10^{-3} M of water was used for the pulse radiolytic study to minimize the effect of water on reaction yields.

20) T. Nakayama, K. Ushida, K. Hamanoue, M. Washio, S. Tagawa, and Y. Tabata, *J. Chem. Soc., Faraday Trans.*, **86**, 95 (1990).

21) In the reaction of the $Ru_3(333)$ system, the formation of the unknown species was not noticed, because the change in absorbance due to the $Ru_3(333)$ reduction was very large.

22) A. M. Koukes-Pujo, B. L. Motais, and L. G. Hubert-Pfarlzgraf, *J. Chem. Soc., Dalton Trans.*, **1986**, 1741.

23) B. L. Motais, A. M. Koukes-Pujo, and L. G. Hubert-Pfarlzgraf, *Radiat. Phys. Chem.*, **29**, 21 (1987).